

# Space charge analysis in quantum well structures leading to spontaneous pulsing

A. G. U. Perera and S. G. Matsik

Department of Physics and Astronomy, Georgia State University, Atlanta, Georgia 30303

(Received 8 May 1995; accepted for publication 16 June 1995)

We present a model describing the basis for spontaneous pulsing behavior in a GaAs/AlAs quantum well structure at 300 K. This model is based on the accumulation of space charge in the well due to tunneling of electrons out of the well leading to a sharp increase in current and hence a pulse. The basic concepts used in the model are verified by comparison with experimental data for a single AlGaAs (or AlAs) barrier between two contacts. These structures will allow the use of neuron-like pulsing phenomena in IR detectors, image processors, neural networks, artificial neurons, etc. at much higher temperatures than the 10 K limit for pulsing observed in silicon *p-i-n* diodes. © 1995 American Institute of Physics.

Spontaneous pulsing has been observed at cryogenic temperatures in circuits containing silicon *p-i-n* diodes driven by a constant voltage source<sup>1</sup> and a constant current source.<sup>2</sup> The circuits display a rich spectrum of both basic physics phenomena and applications. These pulsing structures were used as long wave infrared detectors<sup>3</sup> which do not need any preamplifiers. The similarity of these pulses to the action potentials in biological neurons have led to neuron simulation, including the detection of transient optical signals as in the case of the horseshoe crab eye.<sup>4</sup> By combining two pulsing diode outputs through a filter circuit,<sup>5</sup> a single channel was formed to simulate a photoreceptor channel in a biological retina and, with suitable interconnections among channels, to function as a parallel processor.<sup>6</sup> In addition to these applications, interesting physics/nonlinear dynamics issues have been studied including the observation of Farey fractions,<sup>1</sup> mode locking,<sup>3</sup> transition to chaos.<sup>7</sup>

The use of these applications with *p-i-n* diodes is limited by cooling requirements due to the low temperature at which the pulsing occurs (<10 K). The extension of pulsing to higher temperatures would lead to expanded possibilities for the use of pulsing phenomena. Based on experience with quantum wells<sup>8-11</sup> and pulsing in *p-i-n* structures<sup>12</sup> we are exploring the feasibility of increasing the temperature at which pulsing occurs.<sup>13</sup> This will be accomplished by using the space charge in quantum wells, which is similar to the space charge in the *i*-region of a *p-i-n* diode. A necessary condition for pulsing, *s*-type negative differential conductivity, has been observed in quantum well structures at room temperature.<sup>14</sup> This is a strong indicator that pulsing should be possible at higher temperatures using quantum wells. The primary cause of the temperature limit in *p-i-n* diodes is the thermal ionization of the impurities. The increased ionization leads to a large residual space charge reducing the effects of impact ionization needed for pulsing. The larger binding energy available for electrons in the quantum well should reduce the thermal ionization effects permitting pulses to occur.

The structure proposed for spontaneous pulsing consists of a single quantum well  $\delta$ -doped with silicon between highly doped contacts as shown in Fig. 1(a). The structure is driven by a constant current source as shown in Fig. 1(b). As

charge builds up in the input capacitor, electrons are injected into the device at the load end. These electrons interact with the electrons in the well causing ionization in the well. This leads to an increase in the electric field at the injection contact causing an increased current that leads to a pulse. This discharges the input capacitor and charges the output capacitor. When this occurs the field at the input end of the device changes sign causing electrons to be trapped and neutralizing the charge in the well. The load capacitor then discharges through the load resistance, resetting the system for the next pulse. Throughout the calculations we will use a  $w = 500 \text{ \AA}$  wide GaAs well and 697 meV high ( $\Delta E$ ) AlAs barrier of thickness  $b = 1000 \text{ \AA}$ . [See Fig. 1(a)]. The doping concentration in the well is  $3.75 \times 10^{12} \text{ cm}^{-2}$  and the contacts will be doped to  $1 \times 10^{18} \text{ cm}^{-3}$ . The circuit parameters will be input capacitance  $C = 80 \text{ pF}$ , load capacitance  $C_L = 100 \text{ pF}$  and load resistance  $R_L = 3 \text{ M}\Omega$ .

The calculations involved in this model can be broken down into four parts that are then combined to obtain the

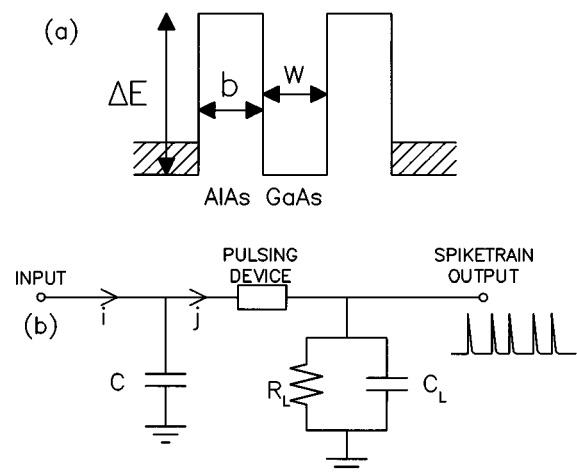


FIG. 1. (a) The structure used in the model. The corresponding parameter values, well width  $w$ , barrier width  $b$ , and barrier height  $\Delta E$  are also shown. (b) The complete circuit used in the analysis. The pulsing device is the quantum well structure.  $C$  is the input capacitor of 80 pF,  $R_L$  and  $C_L$  are the load resistor and load capacitor of 3 M $\Omega$  and 100 pF respectively.

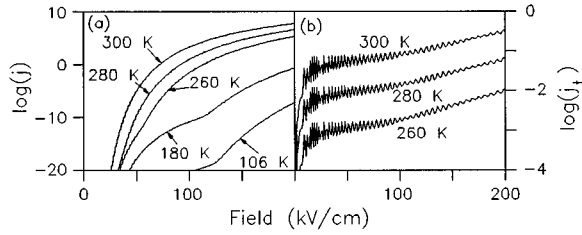


FIG. 2. (a) Injection current as a function of the field across the barrier calculated at 300, 280, 260, 180 and 106 K. (b) Tunneling current as a function of the field in the barrier calculated at 300, 280 and 260 K. The lower temperatures used to compare with the single barrier structure are not calculated here since there is no well for ionization to occur in. The device structure shown in Fig. 1 was used for these calculations. The structure in the curve is due to oscillations in the transmission coefficient.

output pulse. The first part is to determine the fields at the emitter and collector for a given bias and charge in the well. Second, the injected current is calculated as a function of the field at the emitter. Third, the impact ionization rate for electrons in the well is found as a function of the current incident on the well and the number of electrons in the well. Fourth, the tunneling current for electrons out of the well is calculated. The results of these calculations are then combined with the equations for charging the input and load capacitors to produce a system of coupled differential equations that are then integrated numerically to find the output pulse.

The fields at the emitter and collector are given by

$$F_e = \frac{V_i - V_L}{2b + w} + \frac{\sigma}{2\epsilon} \quad (1)$$

$$F_c = \frac{V_i - V_L}{2b + w} - \frac{\sigma}{2\epsilon} \quad (2)$$

respectively, where  $V_i$  and  $V_L$  are the input and load voltages,  $b$  is the barrier width,  $w$  is the well width,  $\sigma$  is the surface charge density in the well and  $\epsilon$  is the permittivity of the well.

The injection current density  $j_{(inj)}$  is calculated from the following equation

$$j_{(inj)} = q \int_0^\infty n_c(E_x) T(E_x, F_e) dE_x \quad (3)$$

where  $q$  is the electron charge,  $n_c$  is the number of electrons per unit area per unit energy per unit time incident on the barrier with energy  $E_x$  and  $T(E_x, F_e)$  is the transmission probability for the incident electrons with energy  $E_x$  and electric field  $F_e$ . We have followed Gundlach<sup>15</sup> for  $T(E_x, F_e)$ . The incident electron distribution is simply the standard Fermi distribution integrated over the directions parallel to the plane of the well giving  $n_c = (4\pi mkT/h^3) \ln(1 + e^{E_x/kT})$ . The integration is then done numerically and the results are shown for varying temperatures in Fig. 2(a). The tunneling current [Eq. (4)] is calculated using the same procedure except that the electron distribution is replaced by the corresponding distribution in the well  $n_w = (4\pi mkT/h^2w) \sqrt{E_i/2m} \ln(1 + e^{(E_i - E_F)/kT})$  where  $E_F$

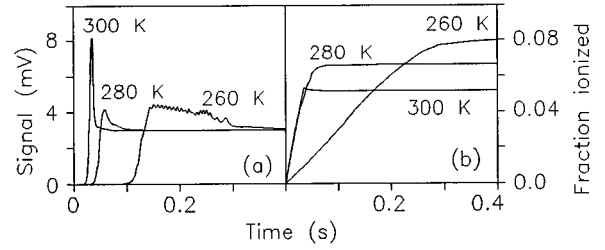


FIG. 3. (a) The calculated output signal showing the spontaneous pulsing and (b) the ionization fraction (space charge in the well) for a GaAs/AlAs quantum well structure with  $w = 500 \text{ \AA}$ ,  $b = 1000 \text{ \AA}$ ,  $n_c = 1.0 \times 10^{18} \text{ cm}^{-3}$  at  $T = 300, 280$  and  $260 \text{ K}$ . The peak in ionization at 300 K indicates a space charge driven pulse. With no clear indication of a space charge peak, the pulse at 280 K is very weak, and at 260 K the structure is trying to pulse but does not succeed in pulsing, producing a wide voltage glitch with time.

is the Fermi energy in the well and  $w$  is the well width. Because the energy levels are now discrete the integral is replaced by the sum

$$j_{(tun)} = q \sum_{i=0}^N n_w(E_i) T(E_i, F_c) \quad (4)$$

where there are  $N + 1$  levels in the well. The results for tunneling current are shown in Fig. 2(b). Both the injection and tunneling currents show oscillations due to resonances in the transmission coefficient.

The impact ionization current was calculated using the method of Chuang and Hess<sup>16</sup> with tunneling of the excited electrons included. This involves integrating the probability of both electrons escaping after a collision of a hot electron with a cold electron in the well over the distribution of electrons. When this was done it was found that the effects of impact ionization are negligible when compared to the tunneling component, so we omit them for the rest of the calculation.

The input ( $C$ ) and load ( $C_L$ ) capacitors obey the following relationships

$$\frac{dV_i}{dt} = \frac{I - jA}{C} \quad (5)$$

$$\frac{dV_L}{dt} = \frac{jA}{C_L} - \frac{V_L}{R_L C_L} \quad (6)$$

where  $I$  is the driving current,  $A$  is the device area,  $C$  and  $C_L$  are the input and load capacitors and  $R_L$  is the load resistor. The final equation needed is the rate of generation of space charge in the well. This is just

$$\frac{d\sigma}{dt} = j_{(tun)}, \quad F_c > 0 \quad (7)$$

$$= -j_{(inj)}, \quad F_c < 0. \quad (8)$$

This system of equations can be integrated numerically with  $V_L$  being the output signal that would be measured experimentally. For the parameters given at 300 K, a pulse is produced as seen in Fig. 3. As the temperature decreases the pulse gets smaller and by 260 K the sharp pulse has dimin-

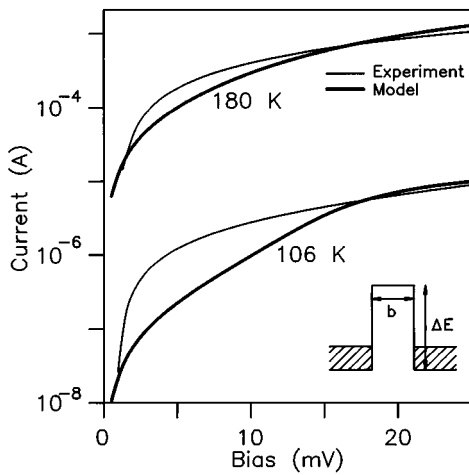


FIG. 4. Experimental and modeling I-V curves for a single barrier structure shown in the inset. The design parameters were  $b=200 \text{ \AA}$  and  $n_c=1.0 \times 10^{18} \text{ cm}^{-3}$ . An Arrhenius plot, considering the Fermi level of 55 meV, gives  $\Delta E=145 \pm 25 \text{ meV}$ . The parameters for the model were  $b=161 \text{ \AA}$ ,  $\Delta E=200 \text{ meV}$  and  $n_c=8.6 \times 10^{17} \text{ cm}^{-3}$ . The two sets of curves are for 180 K and 106 K. The light curve in each set is the experimental data and the heavy curve is the model result.

ished into a wide glitch with extra structure. This extra structure is caused by the oscillations seen in the injection and tunneling currents. Also shown is the fraction of the electrons that have escaped from the well. At 300 K this also shows a maximum indicating that the pulse is being driven by the space charge. At 280 K the space charge increases to a maximum at the pulse but there is no recombination indicating that the transient associated with the input capacitor charging is now becoming important (although space charge is also contributing). At 260 K the space charge is now reaching a steady state after the glitch indicating that it is not generating the glitch in this case but rather the transient associated with charging the input capacitor. For continuous operation the output should return to zero after the pulse. However, in this case the return is to an offset of 3 meV. This is caused by the lack of sufficient electron capture in the recombination phase to reset the structure for the next pulse. Among several possibilities, adjusting the design to increase the injection current during the pulse, leading to an increase in the output voltage and more space charge neutralization would be a major candidate to resolve this issue.

Next, we turn to an experimental test of the model. The I-V curve for a single barrier structure was measured and compared to the output for the model. This simple case is similar to the injection current calculation except the reverse passage of the electrons in the second contact is included. This is done by replacing  $n_c(E_x)$  with  $(n_c(E_x) - n_c(E_x + eV_b))$  in the integral. This calculation was done at 106 K and 180 K. The results are shown in Fig. 4. The single barrier parameters determined by a least squares fit were  $b=161 \text{ \AA}$ ,  $\Delta E=200 \text{ meV}$ , and contact doping of  $8.6 \times 10^{17} \text{ cm}^{-3}$ . These results are within the sample parameters. The design specifications were  $b=200 \text{ \AA}$ ,  $\Delta E=84 \text{ meV}$  and  $n_c=1.0 \times 10^{18} \text{ cm}^{-3}$ . Although the design was for a 84 meV barrier the Arrhenius plot indicates a  $90 \pm 25 \text{ meV}$  barrier. For a concentration  $n_c=1.0 \times 10^{18} \text{ cm}^{-3}$  the Fermi

level is  $\sim 55 \text{ meV}$  giving a  $\Delta E$  of  $145 \pm 25 \text{ meV}$  as a reasonable experimental value. The model results are in reasonable agreement with the experimental data at both temperatures, supporting the results of this calculations. The deviation at low bias in the 106 K case may be due to the presence of an assisting mechanism for the injection such as phonon assisted tunneling which is not considered here. Since the tunneling current uses the same procedure this also provides evidence of its validity.

These structures may prove useful as IR detectors when operated at a reduced temperature. The rate of generation of space charge is sensitive to the population distribution of electrons in the well. Reducing the temperature reduces the population in the higher energy levels that contribute to the tunneling, leading to reduced space charge generation rates. This can preclude pulsing until the presence of IR radiation increases the population in the higher energy levels back to that at the spontaneous pulse operating temperature. Thus pulsing occurs only when IR radiation is incident on the structure.

In conclusion, we have presented a model establishing conditions for spontaneous pulsing in a GaAs/AlGaAs quantum well structure at 300 K this pulse is the result of the accumulation of space charge in the well leading to an increase in the output current. The model has been tested by comparison with experimental data from a single barrier structure confirming the basic features of the model.

This work was supported in part by the NSF under grant #9412248. The single barrier sample was grown at Cornell by Dr. William Schaff and the sample processing was done at NRC-Canada by Dr. H. C. Liu.

- <sup>1</sup>D. D. Coon, S. N. Ma, and A. G. U. Perera, Phys. Rev. Lett. **58**, 1139 (1987).
- <sup>2</sup>D. D. Coon and A. G. U. Perera, Appl. Phys. Lett. **55**, 478 (1989).
- <sup>3</sup>D. D. Coon and A. G. U. Perera, Appl. Phys. Lett. **51**, 1086 (1987).
- <sup>4</sup>A. G. U. Perera, S. Betarbet, and M. H. Francombe, *Multispectral Transient Sensing based on Retinal concepts in a Parallel Processor*, in WCNN 93 Portland (Lawrence Erlbaum Associates, NJ, 1993), pp. IV 835-IV 838.
- <sup>5</sup>A. G. U. Perera, S. R. Betarbet, and S. G. Matsik, "Bifurcations and Chaos in Pulsing Si Neurons," in *World Congress on Neural Networks (WCNN 94 San Diego)*, Lawrence Erlbaum Associates, NJ, 1994, p. IV 704.
- <sup>6</sup>D. D. Coon and A. G. U. Perera, "Photon Detection with Parallel Asynchronous Processing," in *Visual Communications and Image Processing '90-SPIE Vol. 1360*, (SPIE, 1990), pp. 1620-1630.
- <sup>7</sup>A. G. U. Perera and S. G. Matsik, Physica D **84**, 615 (1995).
- <sup>8</sup>B. F. Levine, J. Appl. Phys. **74**, R1 (1993).
- <sup>9</sup>S. D. Gunapala, B. F. Levine, and N. Chand, J. Appl. Phys. **70**, 305 (1991).
- <sup>10</sup>H. C. Liu, Appl. Phys. Lett. **61**, 2703 (1992).
- <sup>11</sup>A. G. U. Perera, "Evidence for LWIR Emission Using Intersubband Transitions in GaAs/AlGaAs MQW Structures," in *Quantum Well Intersubband Transition Physics and Devices* (Kluwer Academic, Norwell, MA, 1994), pp. 525-532.
- <sup>12</sup>A. G. U. Perera and S. Matsik, Appl. Phys. Lett. **64**, 878 (1994).
- <sup>13</sup>S. G. Matsik and A. G. U. Perera, Bull. Am. Phys. Soc. **39**, 857 (1994).
- <sup>14</sup>Zh. I. Alferov et al., Sov. Phys. Semicond. **21**, 304 (1987).
- <sup>15</sup>K. H. Gundlach, Solid State Electron. **9** 949 (1966).
- <sup>16</sup>S. L. Chuang and K. Hess, J. Appl. Phys. **61**, 1510 (1987).